Estimation of wheat plant area index and plant area distribution from terrestrial LiDAR

Raul Lopez Lozano, Tian Ma, Maxime Soma, Aurélien Ausset, Bruno Berthon, Philippe Burger, Romain Chapuis, Marie-Pia D'Argaignon, Antonin Grau, Florian Larue, et al.

Estimation of Plant Area Index and Plant Area Distribution from Terrestrial LiDAR

R. Lopez-Lozano[1], T. Ma[1], M. Soma[2], A. Ausset[3], B. Berthon[4], F. Burger[3], R. Chapuis[4], M.P. D'Argaignon[1], A. Grau[4], F. Larue[3], R. Le-Roy[4], R. Marandel[5], V. Mercier[1], M. Roy[5], G. Tison[5], F. Venault[1], M. Weiss[1], P. Martre[3], F. Baret[1]

[1] INRAE, Avignon Université, UMR EMMAH, Avignon (France)
[2] INRAE, Aix-Marseille Université, UMR RECOVER, Aix-en-Provence (France)
[3] INRAE, Univ Montpellier, Institute Agro, UMR LEPSE, Montpellier (France)
[4] INRAE, UE DiaScope, Mauguio (France)
[5] INRAE, UE APC, Auzeville (France)

INRAE

anr
Agence National de la Recherche

Introduction: Plant Area Index from LiDAR

Light **D**etection **A**nd **R**anging

Essentially, a method to measure distances

A light beam is emitted in the direction θ …

…the beam is reflected back from the canopy. The **difference in time, or phase** of the reflected signal permits to **determine the distance** to the impact

A large number of beams permits to produce a point cloud of the object observed

On species with **large leaves and simple architecture**, **mesh reconstruction** can provide an estimation of leaf/plant area…

… but what about **complex/dense canopies**?

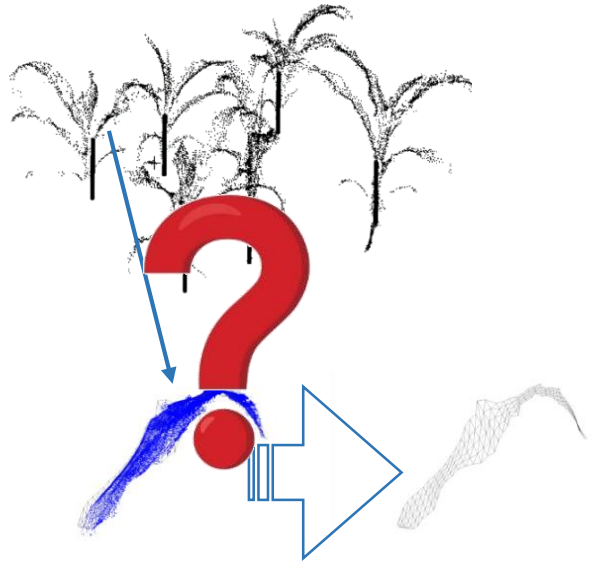

Objectives

1) Developing a **methodology to estimate the** 3D **distribution of Plant Area Index** (PAI: leaves + stems + ears, green or not) suitable for wheat canopies **from LiDAR point clouds**

2) **Assessing such methodology** in actual field experiments (canopy PAI)

3) **Understanding the role of different factors** (e.g. LiDAR viewing configurations, hypothesis on leaf inclination) **in the accuracy of PAI estimations**

INRAE

Materials & methods: Field trials

3 Field trials in the south of France (FFAST project, funded by ANR)

DiaPhen platform at Mauguio (near Montpellier) in 2022 and 2023
AgroPhen at Auzeville (near Toulouse) in 2023

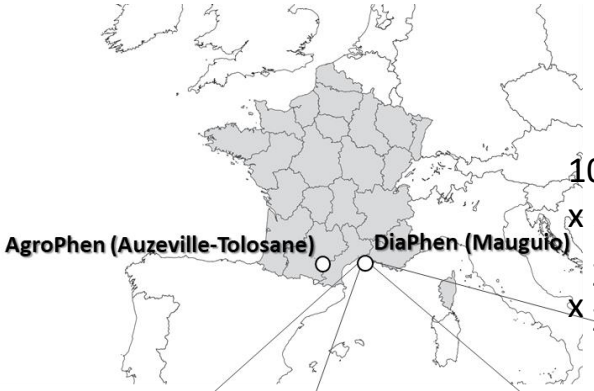

Cultivar	Registration year	Cold requirement[a]	Precocity at stem extension[b]	Precocity at heading[b]	Height[c]	Awn	Genetic panel[d]
Renan	1990	1	1	6	4	Yes	WH
Fructidor	2014	2	3	6	3.5	Yes	BW
Rubisco	2012	3	3	6.5	3	No	BW, SA, IN
Nemo	2015	3	3	6.5	3.5	Yes	BW
LG Absalon	2016	3	3	6.5	3.5	No	SA, IN
Chevignon	2017	3	2	6	4	No	IN
Apache	1998	4	3	7	3.5	No	BW, SA, IN, WH
RGT Sacramento	2014	4	6	6.5	3.5	Yes	IN
Oregrain	2012	5	4	7	3.5	No	BW, SA, IN
Nogal	2006	8	5	8	3.5	Yes	BW, SA, IN

[a] 1: very winter, 9: very spring; [b] 1: late, 9: early; [c] 1: very short, 9: very tall; [d] included in previous projects: BW: ANR PIA Breedwheat, SA: H2020 SolACE, WH: FP7 Whealbi, IN: H2020 INVITE.

10 Genotypes
x 2 sowing dates
2 water treatments (DiaPhen)
x 2 sowing densities (AgroPhen)

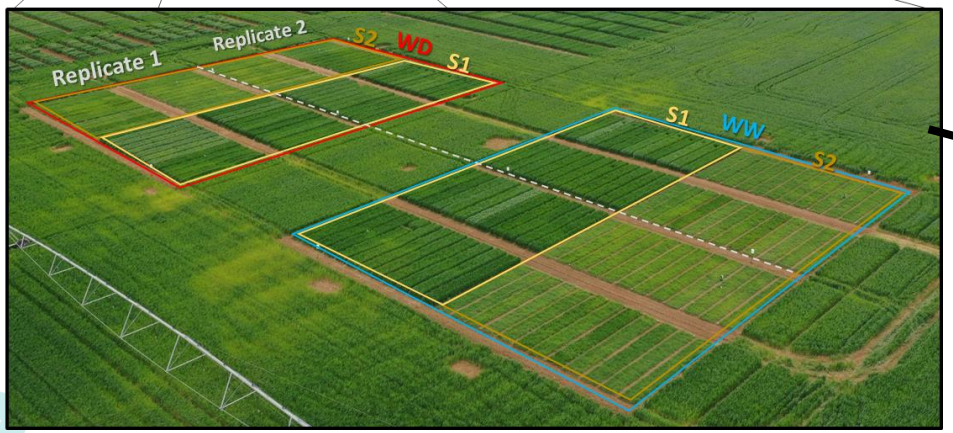

FFAST trial at DiaPhen (Mauguio) 2023

Collection of 292 destructive PAI at different growth stage both years

Site	Date Phenomobile	Date manual sampling	Nb. samples	Growth stage
DiaPhen (Mauguio)	28/03/2022	29/03/2022	40	BBCH31 (S1) BBCH23 (S2)
	26/04/2022	27/04/2022	36	BBCH39 (S1) BBCH31 (S2)
	18/05/2022	19/05/2022	19	BBCH39 (S2)
	17/04/2023	18/04/2023	40	BBCH39 (S1) BBCH31 (S2)
	09/05/2023	10/05/2023	20	BBCH65 (only S1)
	14/05/2023	15/05/2023	20	BBCH65 (only S2)
AgroPhen (Auzeville)	20/03/2023	21/03/2023	39	BBCH31 (S1) BBCH23 (S2)
	19/04/2023	20/04/2023	20	BBCH39 (only S1)
	03/05/2023	03/05/2023	20	BBCH39 (only S2)
	09/05/2023	10/05/2023	19	BBCH65 (only S1)
	22/05/2023	23/05/2023	19	BBCH65 (only S2)

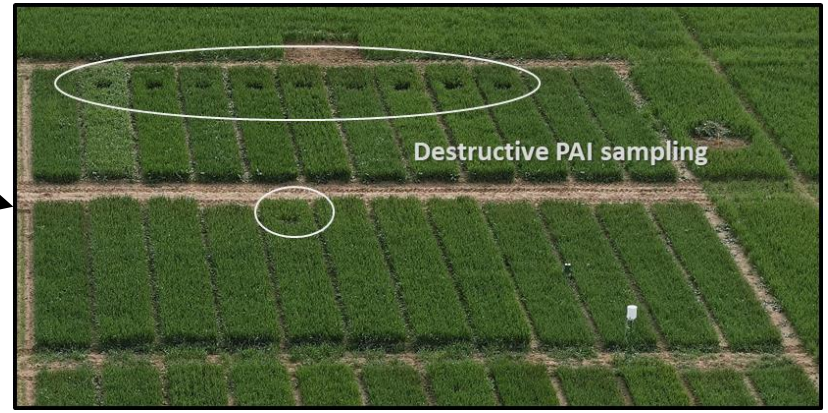

Materials & methods: LiDAR point clouds

LiDAR point clouds were collected with the **Phenomobile V2 ground robot**

3-LiDAR system (SICK LMS 4124)

FOV : 70°
Angular resolution of 0.0833°
Range: 5.5 meters
Scanning frequency: 600 Hz

Point clouds ~30 M points per 10 m^2 microplot

Mesurement head
equipped with RTK GPS
and Inertial Unit

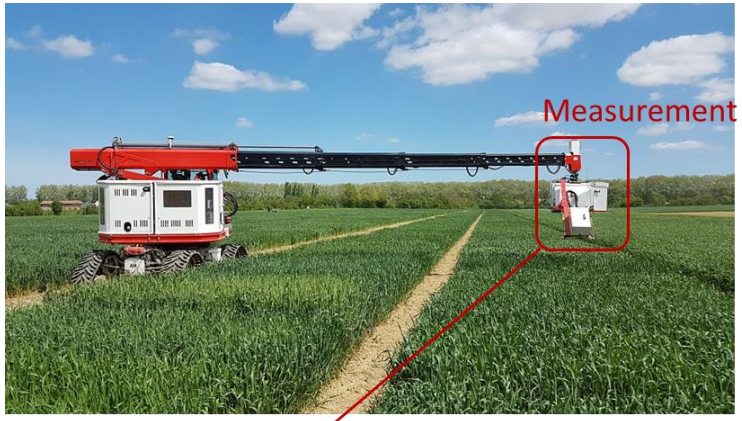

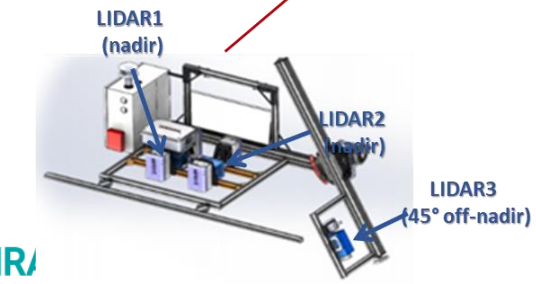

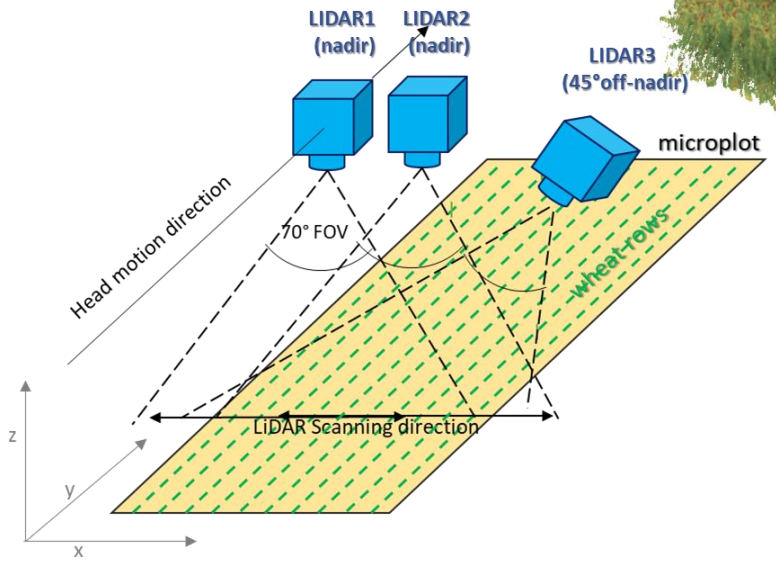

Materials & methods: Estimation of PAI (I)

Original LiDAR point-clouds

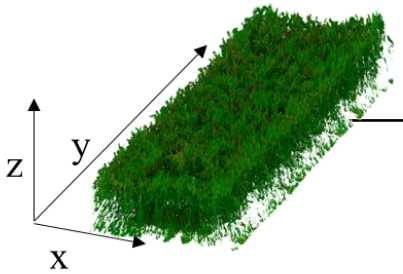

Ground plane detection

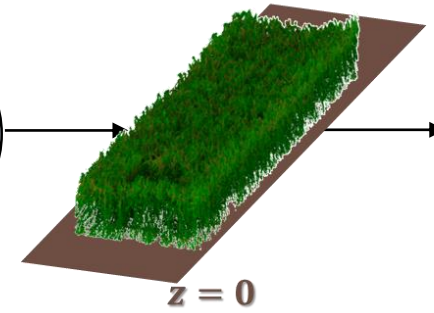

Based on the frequency of LiDAR 1 and 2 impacts in the z-direction.

Linear model fitted using a sliding window along the y-direction

Offset of 3.5 cm above the ground line due to soil roughness

Voxel definition

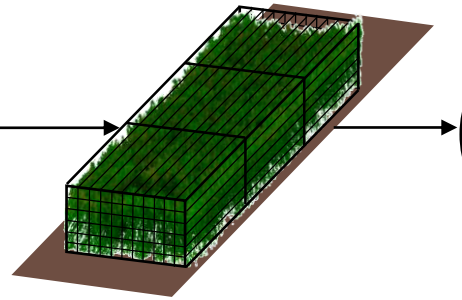

voxels dimensions in x and z dimensions are 1/10 of the row spacing (10 voxels = 1 complete interrow)

voxels dimensions in the y dimensions is 0.5 meters (↑ beams/voxel)

Computation of voxel gap fraction $P_{0,v}$

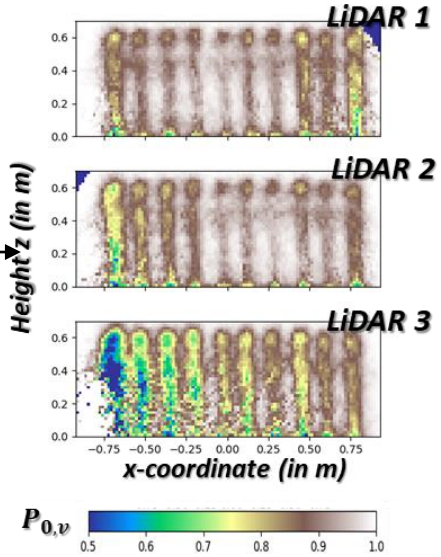

Beams counting

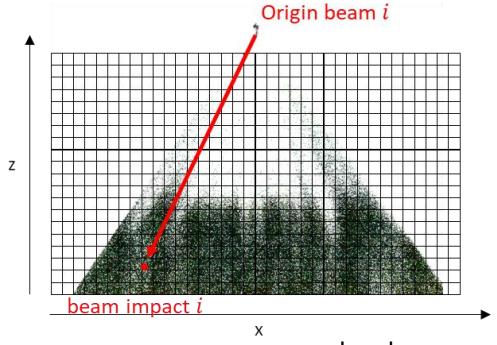

$$P_{0,v} = \frac{|I_{\downarrow,v}|}{|I_{\uparrow,v}|}$$

$I_{\downarrow,v}$ number of beams passing through voxel v

$I_{\uparrow,v}$ number of incident beams in voxel v

Materials & methods: Estimation of PAI (II)

Voxel gap fraction

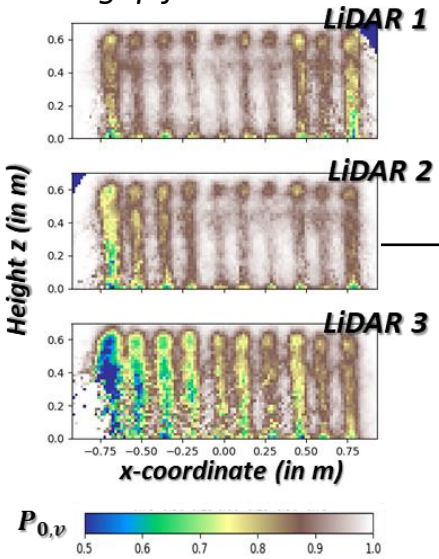

Retrieval of PAI and AIA

Assumptions:

- ***AIA* is the same for all voxels at height *z*** : AIA_z,
- but ***PAI* varies from voxel to voxel** : PAI_v

1) for every z, **sample AIA_z** from 0° to 90°

2) **for a given AIA_z, compute the optimal PAI_v** per voxel is retrieved by solving the linear model:

$$\log(\overrightarrow{P_{0,v}}) = -\overrightarrow{k(AIA_z)_v} * PAI_v$$

3) For all voxels in z, **select the AIA_z** value that yields the best fit to the observed gap fraction vector, so **that mimizes:**

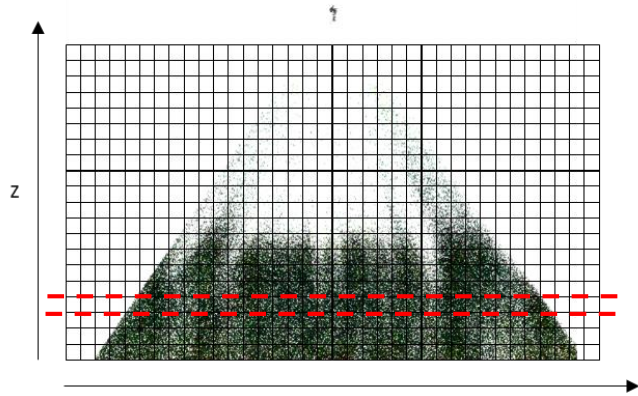

$$J(AIA_z) = \sum \left(\overrightarrow{P_{0,v}} - \overrightarrow{P'_{0,v}(AIA_z)}\right)^2$$

where

$$\overrightarrow{P'_{0,v}(AIA_z)} = e^{-PAI_v * \overrightarrow{k(AIA_z)_v}}$$

Inversion of Beer-Lambert (BL) law at the voxel level

$$P_{0,v} = e^{-PAI_v * k} \quad \text{where} \quad k = \frac{G(\theta_i, AIA)}{\cos\theta_i}$$

PAI_v is the voxel PAI (m² plant area / m² of the voxel side area)

k is the extinction coefficient

2 unkowns

$G(\theta_i)$ is the gamma-function that projects in the zenith angle θ_i a unit of plant area inclined following a distribution given by AIA

AIA is the average inclination angle (°) from Campbell, (1986) ellipsoidal model

but…

how?

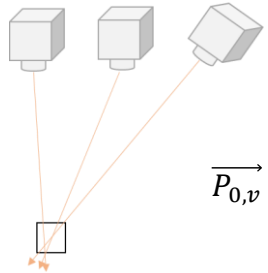

$$\overrightarrow{P_{0,v}} = \begin{bmatrix} P_{0,v,LiDAR1} \\ P_{0,v,LiDAR2} \\ P_{0,v,LiDAR3} \end{bmatrix} \qquad \overrightarrow{k_v} = \begin{bmatrix} \frac{G(\theta_{LiDAR1}, AIA)}{\cos\theta_{LiDAR1}} \\ \frac{G(\theta_{LiDAR2}, AIA)}{\cos\theta_{LiDAR2}} \\ \frac{G(\theta_{LiDAR3}, AIA)}{\cos\theta_{LiDAR3}} \end{bmatrix}$$

The **same voxel is observed by three LiDAR** at different viewing angles, which makes **possible to invert BL numerically**

Materials & methods: Estimation of PAI (III)

Voxel gap fraction

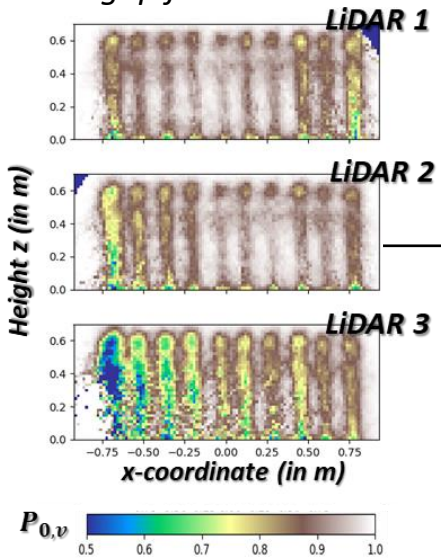

Retrieval of PAI and AIA

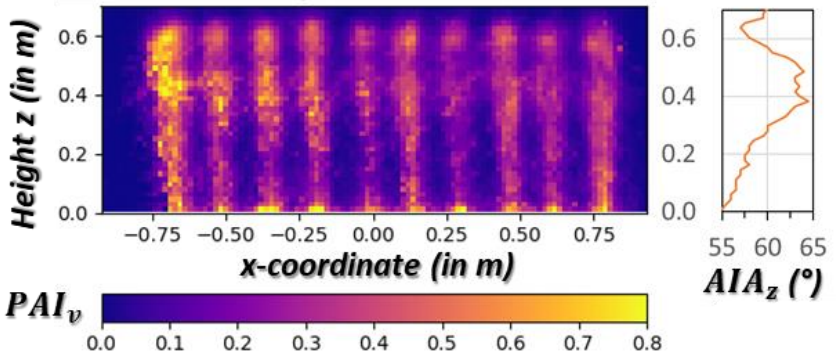

Inversion of Beer-Lambert (BL) law at the voxel level

$$P_{0,v} = e^{-PAI_v * k} \quad \text{where} \quad k = \frac{G(\theta_i, AIA)}{\cos\theta_i}$$

We tested different hypothesis

2 viewing configurations:

3 LiDAR vs 2 LiDAR

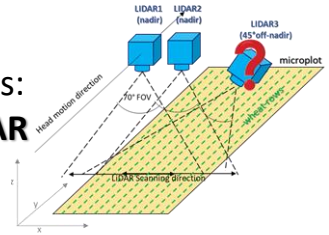

3 hypothesis on ***AIA***

a) AIA unconstrained (free) $$J(AIA_z) = \sum \left(\overrightarrow{P_{0,v}} - \overrightarrow{P'_{0,v}(AIA_z)}\right)^2$$

b) AIA constrained (penalty term) Demarez et al., (2008) $$J(AIA_z) = \sqrt{\sum \left(\frac{\overrightarrow{P_{0,v}} - \overrightarrow{P'_0(AIA_z)}}{\sigma_{P_0}}\right)^2 + \left(\frac{AIA_z - ALA_\mu}{ALA_\delta}\right)^2}$$

c) AIA = 60° (spherical model) $$\log\left(\overrightarrow{P_{0,v}}\right) = -\overrightarrow{k(60°)_v} * PAI_v$$

Materials & methods: validation of canopy PAI

Voxel gap fraction

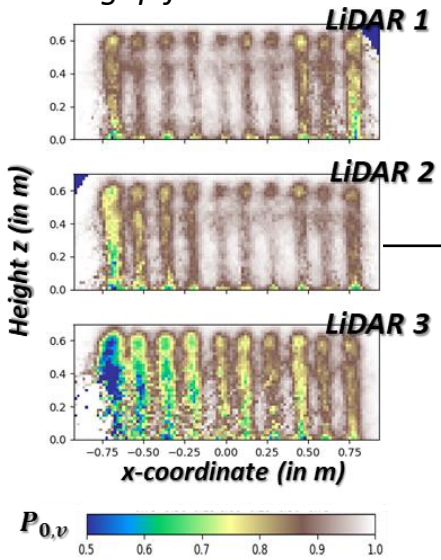

Retrieval of PAI and AIA

Compute canopy PAI from voxels overlapping with the area sampled destructively

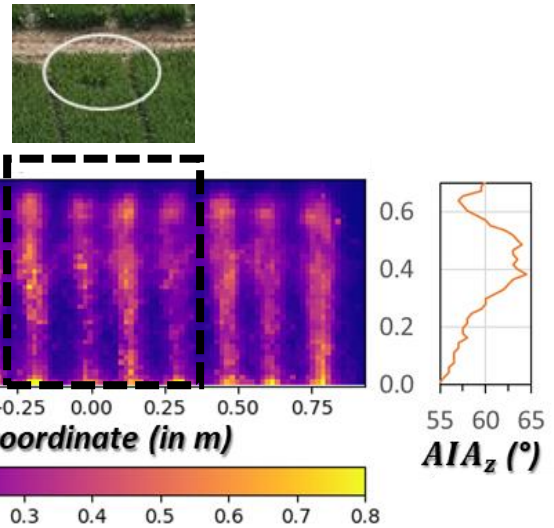

Inversion of Beer-Lambert (BL) law at the voxel level

$$P_{0,v} = e^{-PAI_v * k} \quad \text{where} \quad k = \frac{G(\theta_i, AIA)}{\cos\theta_i}$$

We tested different hypothesis

2 viewing configurations:
3 LiDAR vs 2 LiDAR

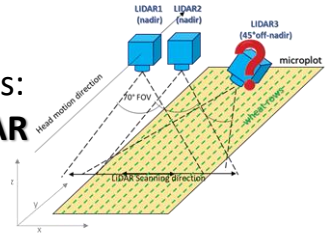

3 hypothesis on ***AIA***

a) AIA unconstrained (free)

$$J(AIA_z) = \sum \left(\overrightarrow{P_{0,v}} - \overrightarrow{P'_{0,v}(AIA_z)}\right)^2$$

b) AIA constrained (penalty term) Demarez et al., (2008)

$$J(AIA_z) = \sqrt{\sum \left(\frac{\overrightarrow{P_{0,v}} - \overrightarrow{P'_0(AIA_z)}}{\sigma_{P_0}}\right)^2 + \left(\frac{AIA_z - \boldsymbol{ALA_\mu}}{\boldsymbol{ALA_\delta}}\right)^2}$$

c) AIA = 60° (spherical model)

$$\log\left(\overrightarrow{P_{0,v}}\right) = -\overrightarrow{k(60°)_v} * PAI_v$$

Results – Accuracy of canopy PAI

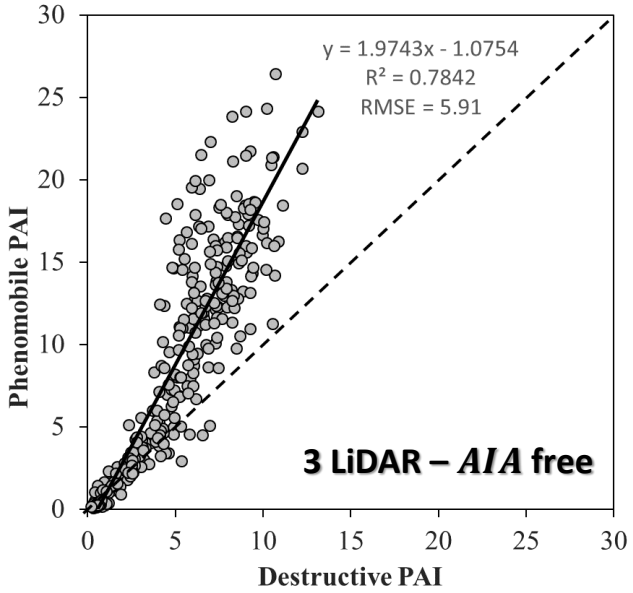

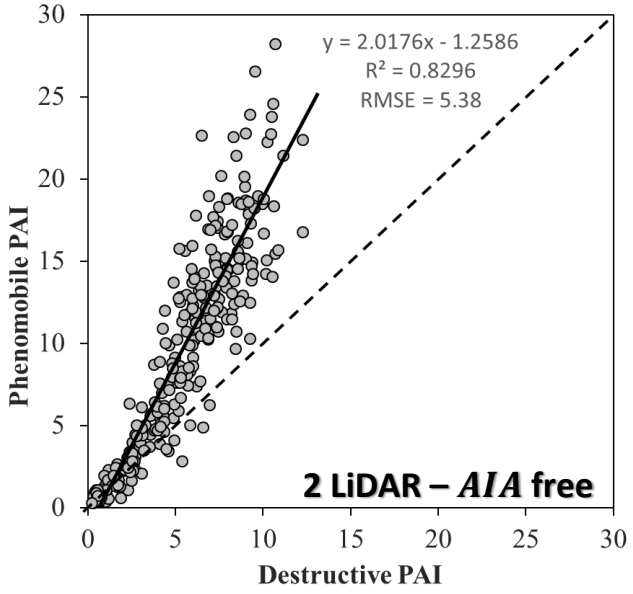

Large overestimation of *PAI* when no prior information **on *AIA*** is given in the inversion of BL

Need to constrain *AIA* to achieve satisfactory results

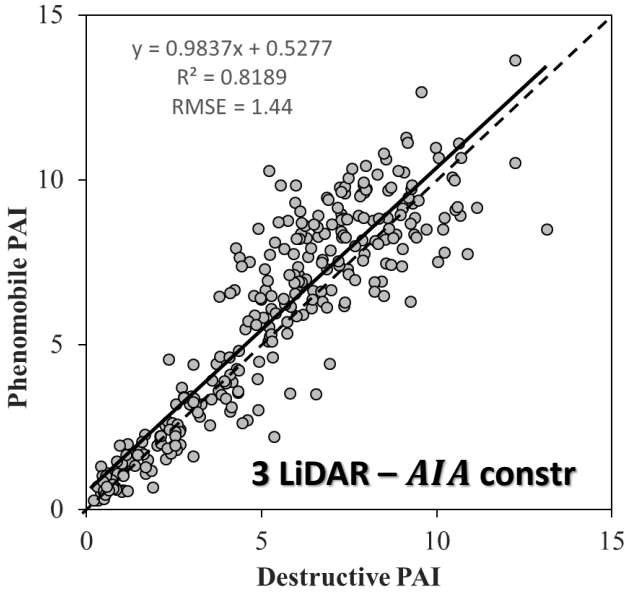

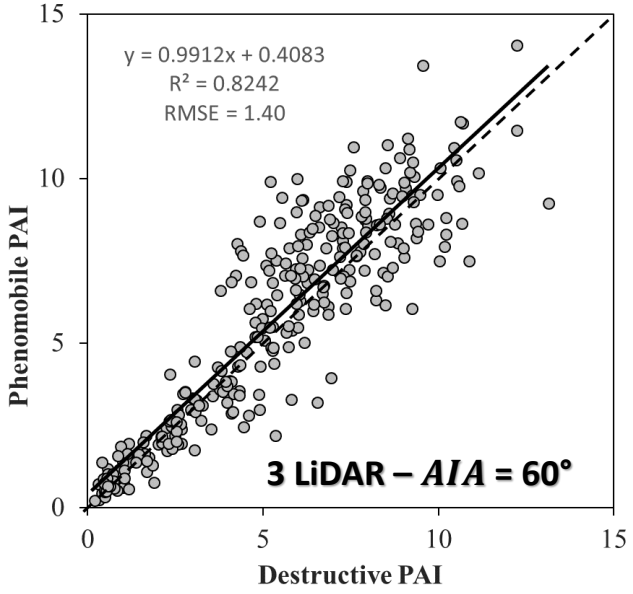

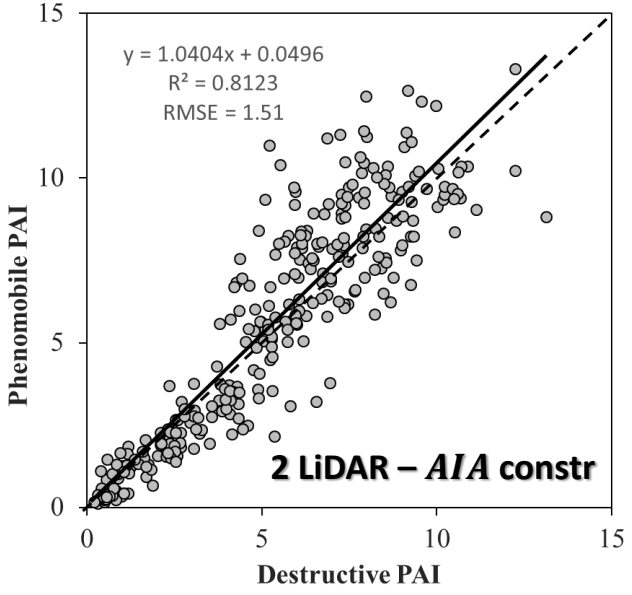

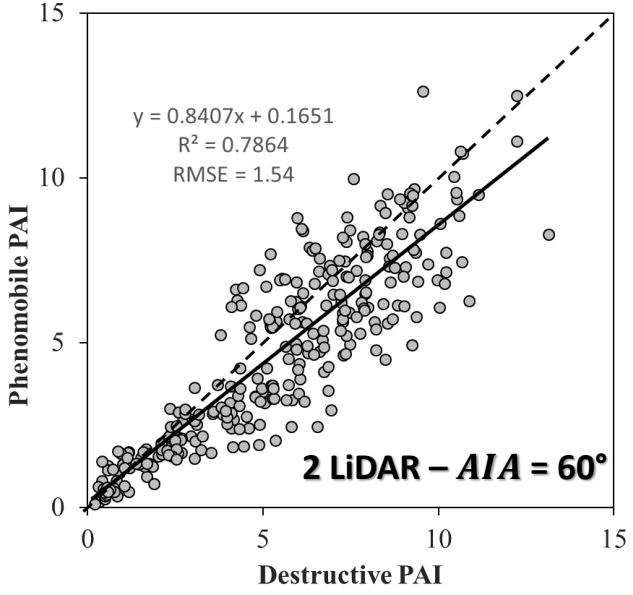

Results – Accuracy of canopy PAI – impact of inclination angle

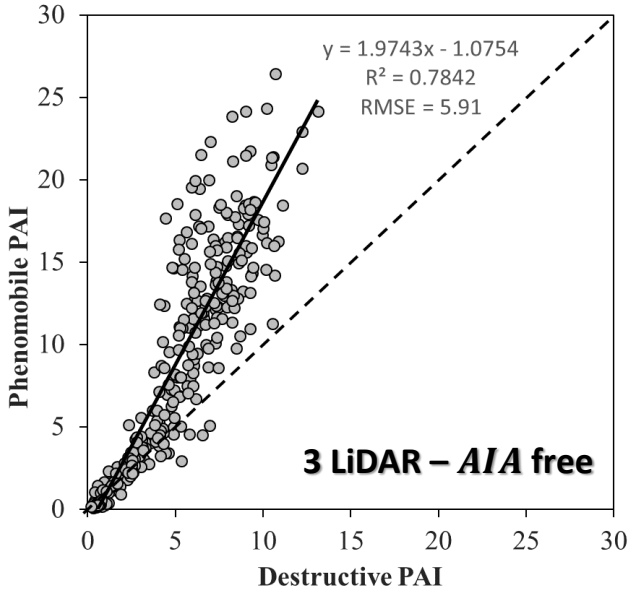

Large overestimation of PAI when no prior information **on AIA** is given in the inversion of BL

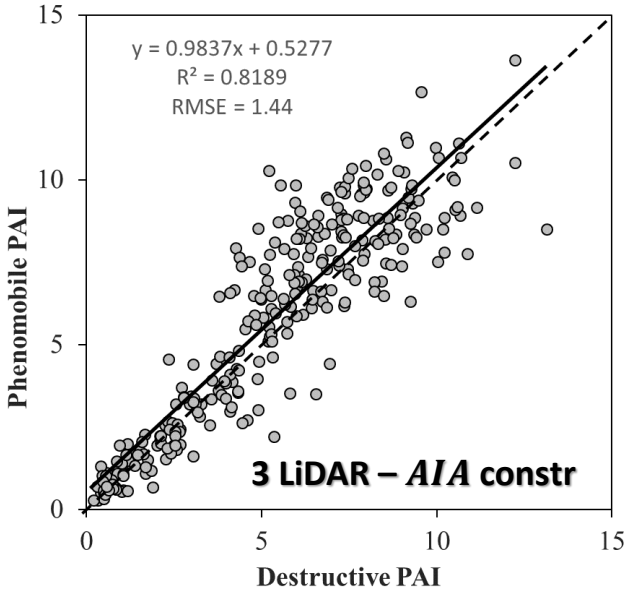

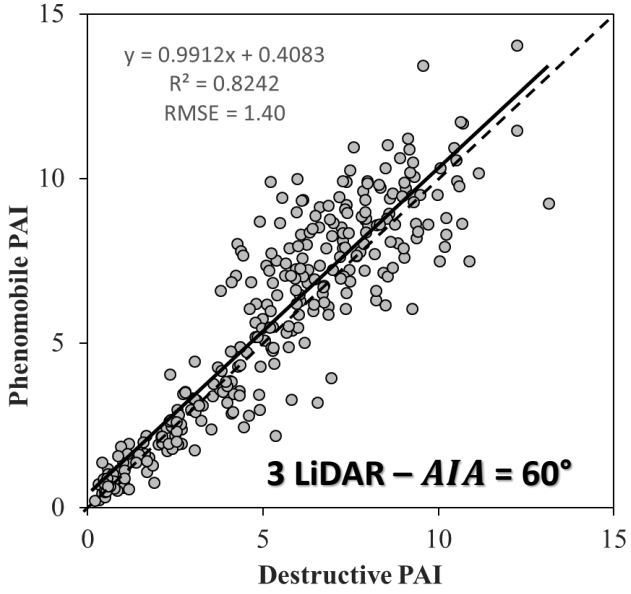

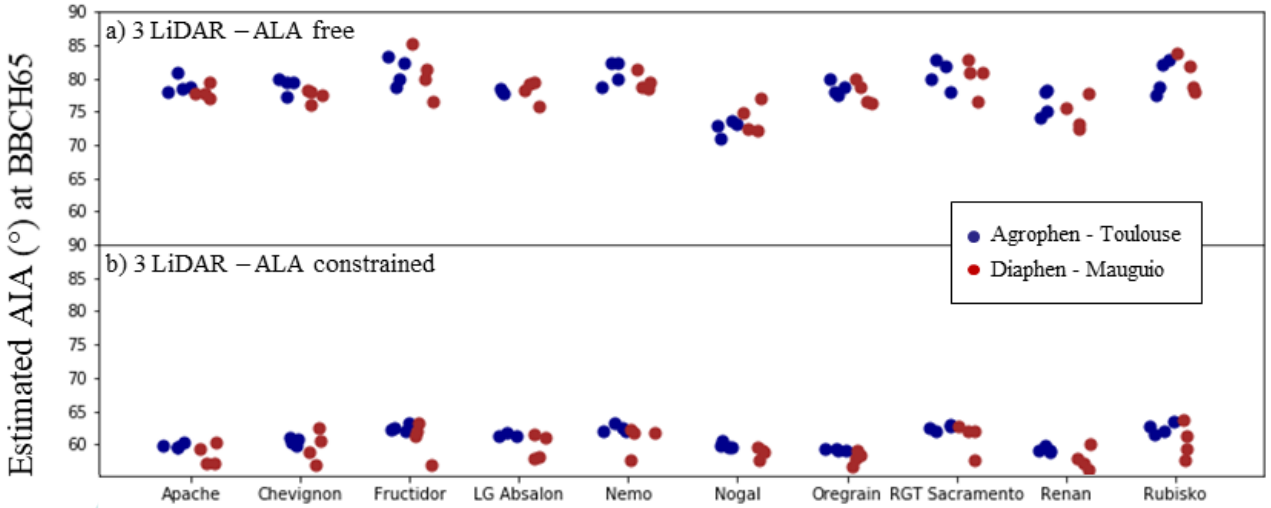

The biased PAI for AIA free is **due to unrealistically high AIA**

Reason: slight bias in $P_{0,v}$ due to the LiDAR spot size

The penalty term permits to restrict the variation of AIA around the expected value of 60°

$$J(AIA_z) = \sqrt{\sum \left(\frac{\overrightarrow{P_{0,v}} - \overrightarrow{P'_0(AIA_z)}}{\sigma_{P_0}} \right)^2 + \left(\frac{AIA_z - \boldsymbol{ALA_\mu}}{\boldsymbol{ALA_\delta}} \right)^2}$$

Results –Impact of inclination angle

Effect of the values of the penalty term parameters in the RMSE

Adapting AIA_μ and AIA_δ permits the estimated AIA to vary across genotypes, dates and height…

… but resulting in the same RMSE as fixing AIA to 60°

Can we just keep fixed AIA?

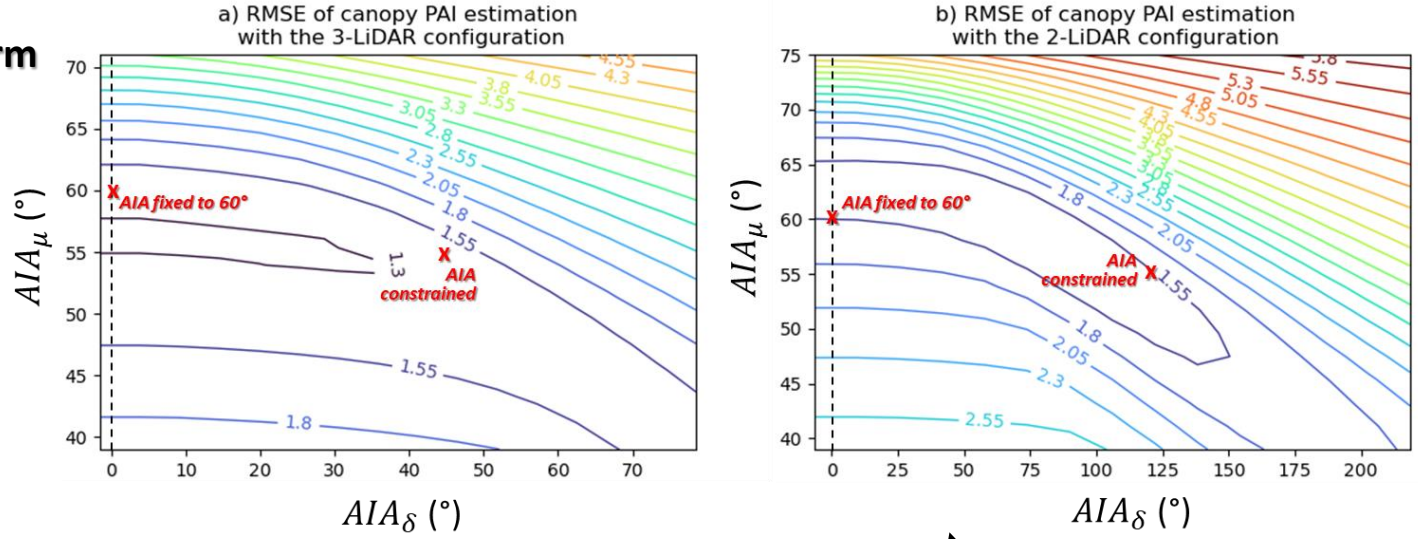

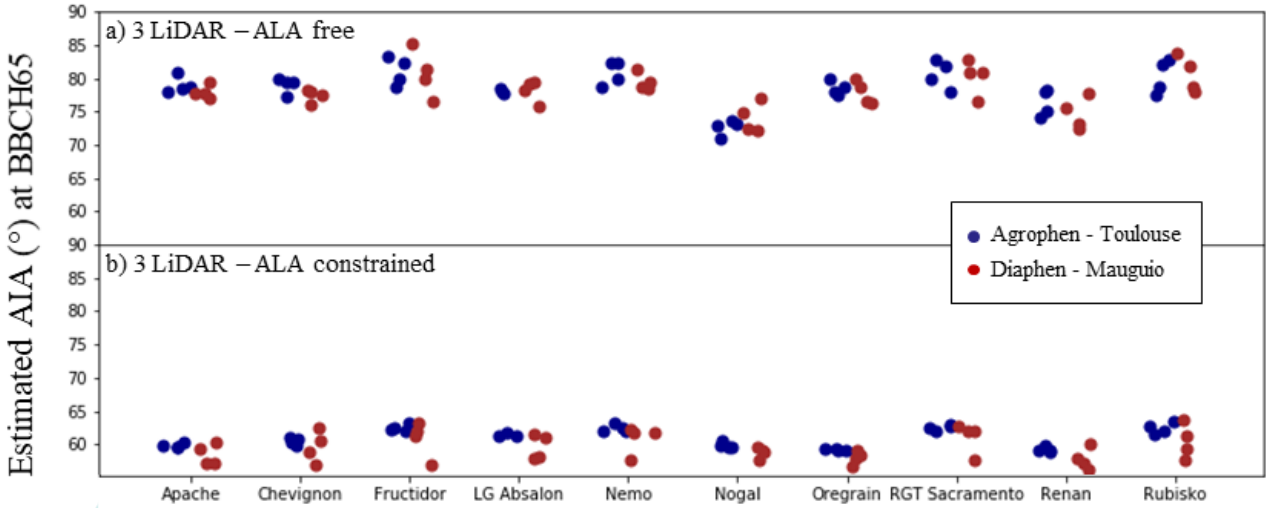

The biased PAI for AIA free is **due to unrealistically high AIA**

Reason: slight bias in $P_{0,v}$ due to the LiDAR spot size

The penalty term permits to restrict the variation of AIA around the expected value of 60°

$$J(AIA_z) = \sqrt{\sum \left(\frac{\overrightarrow{P_{0,v}} - \overrightarrow{P'_0(AIA_z)}}{\sigma_{P_0}} \right)^2 + \left(\frac{AIA_z - AIA_\mu}{AIA_\delta} \right)^2}$$

Results – Variability of inclination angle

Can we just keep the inclination angle AIA fixed?

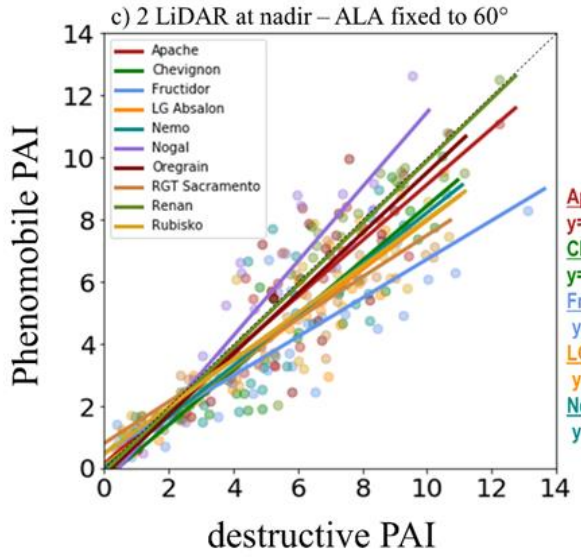

Linear correlation between estimated and destructive canopy PAI per cultivar

Apache: y=0.90x + 0.14; R^2 = 0.87; n=30
Chevignon: y=0.88x - 0.36; R^2 = 0.87; n=30
Fructidor: y=0.62x + 0.50; R^2 = 0.77; n=30
LG Absalon: y=0.79x + 0.09; R^2 = 0.86; n=27
Nemo: y=0.82x + 0.01; R^2 = 0.75; n=30
Nogal: y=1.20x - 0.53; R^2 = 0.84; n=30
Oregrain: y=0.97x - 0.22; R^2 = 0.80; n=29
RGT Sacramento: y=0.67x + 0.80; R^2 = 0.83; n=30
Renan: y=1.0x - 0.11; R^2 = 0.94; n=28
Rubisko: y=0.76x + 0.46; R^2 = 0.88; n=29

Especially at nadir-viewing (2 LiDAR), **fixing AIA leads to differences in** estimated canopy **PAI among the cultivars**

The third LiDAR helps to mitigate it (not shown), but not fully

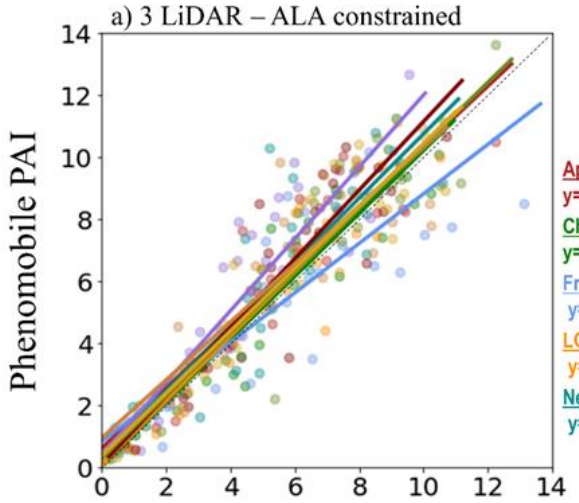

Apache: y=0.97x + 0.62; R^2 = 0.86; n=30
Chevignon: y=1.01x + 0.07; R^2 = 0.87; n=30
Fructidor: y=0.80x + 0.84; R^2 = 0.72; n=30
LG Absalon: y=1.04x + 0.09; R^2 = 0.89; n=27
Nemo: y=1.04x + 0.40; R^2 = 0.78; n=30
Nogal: y=1.16x + 0.41; R^2 = 0.79; n=30
Oregrain: y=1.11x + 0.09; R^2 = 0.84; n=29
RGT Sacramento: y=0.94x + 0.95; R^2 = 0.80; n=30
Renan: y=1.01x + 0.29; R^2 = 0.89; n=28
Rubisko: y=1.01x + 0.38; R^2 = 0.88; n=29

Allowing AIA to vary using the penalty term in the AIA constrained hypothesis **keeps the accuracy** of PAI more **stable across cultivars**

It mitigates the impact on PAI of the actual **differences in leaf inclination** across the cultivars

Results - Leaf inclination differences across cultivars

Estimated AIA per cultivar at flowering (BBCH65) in the two experimental sites

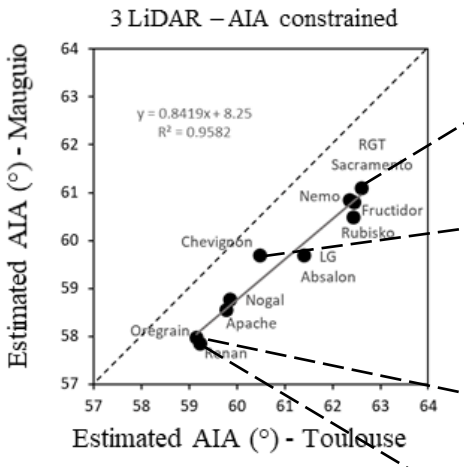

The **differences** in *AIA* **across cultivars are coherent in both sites**

Are these differences due to actual differences in leaf inclination?

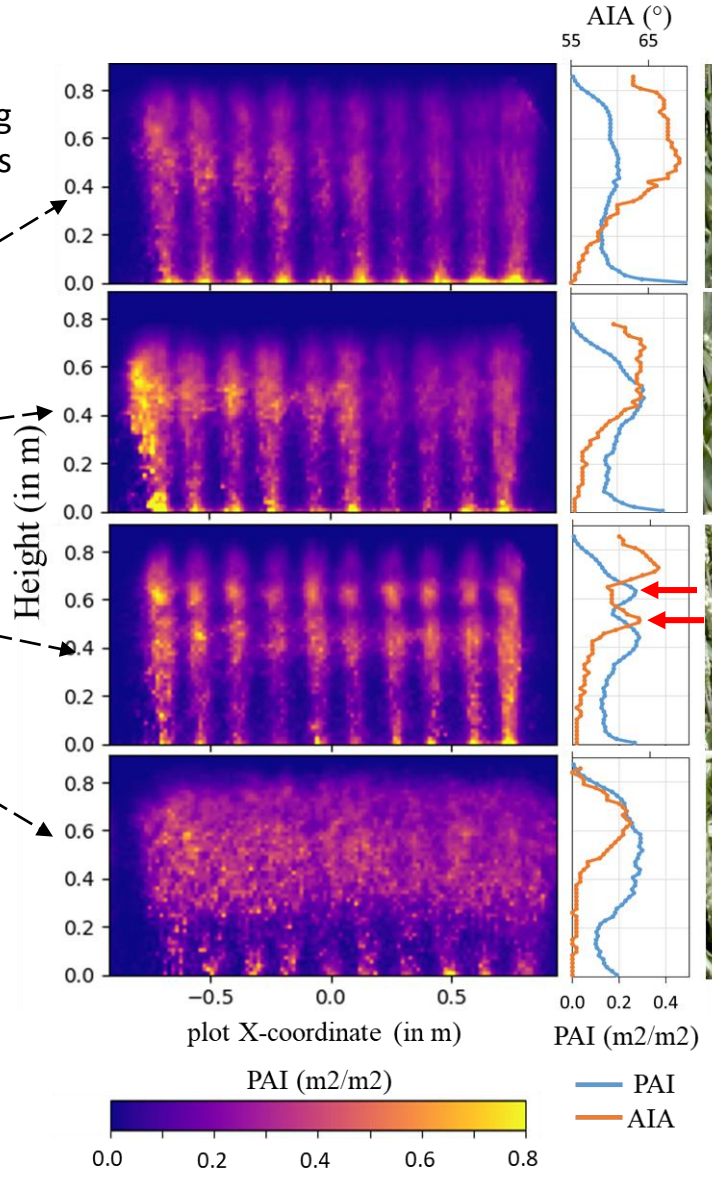

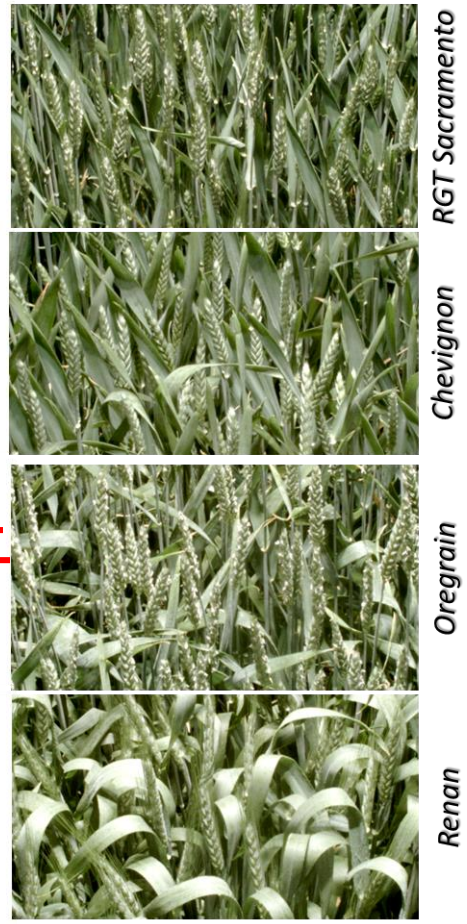

RGT Sacramento has a more erectophile habit (~70°) in the upper half of the canopy

Chevignon has an intermediate AIA (~65° inclination)

Flag leaves of Oregrain have a planophile habit…

…that permit to see the average insertion height and the mid of of the last internode

Renan has large, curved leaves, decreasing AIA which do not permit to appreciate the row structure in the upper half

This suggests that the **estimated AIA describes** the actual variability of **leaf inclination across cultivars in relative terms**

But **we cannot evaluate the absolute accuracy** of the estimated AIA

Conclusions and perspectives

We proposed a **method suited for dense canopies to estimate** canopy PAI and to describe **the 3D variability of plant area index (PAI)** and the **average inclination angle (AIA),** based in the inversion of Beer-Lambert law at the voxel-level

The **validation of canopy PAI** estimations against destructive measurements showed **satisfactory results**, but highlighted the **need to have some prior knowledge on AIA**

Constraining AIA with a penalty term to the inversion **seems the best option** to prevent the impact of actual differences in leaf inclinations in PAI accuracy, **but the penalty term is *a priori* instrument-dependent**

The **estimated AIA describes** well the **relative** variability of **leaf inclination** of actual cutivars, but **it is difficult to validate in absolute terms** with field observations

The future challenge is **extracting more detailed organ-level traits from** the **spatial PAI** information provided by LiDAR

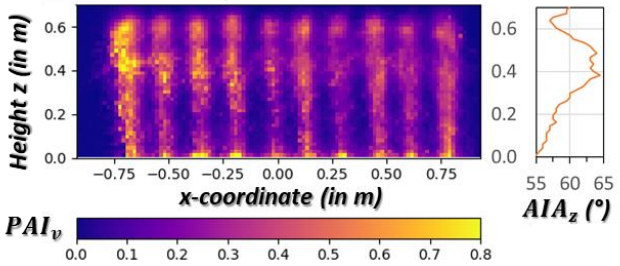

Acknowledgments







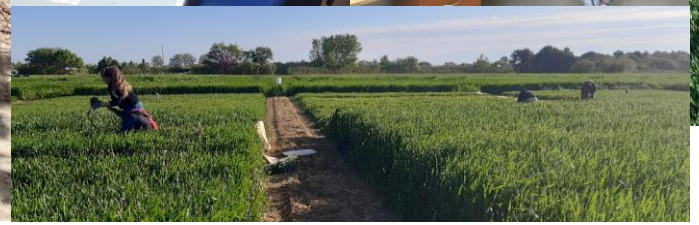

This study has been funded by the ANR (French National Research Agency) through the project FFAST (Functioning from the Assimilation of Structural Traits), project number ANR-21-CE45-0037

INRAE

Bonus track: In silico valiation

Evaluation in silico of the proposed methodology over 3D scenes simulated with the AdelWheat model

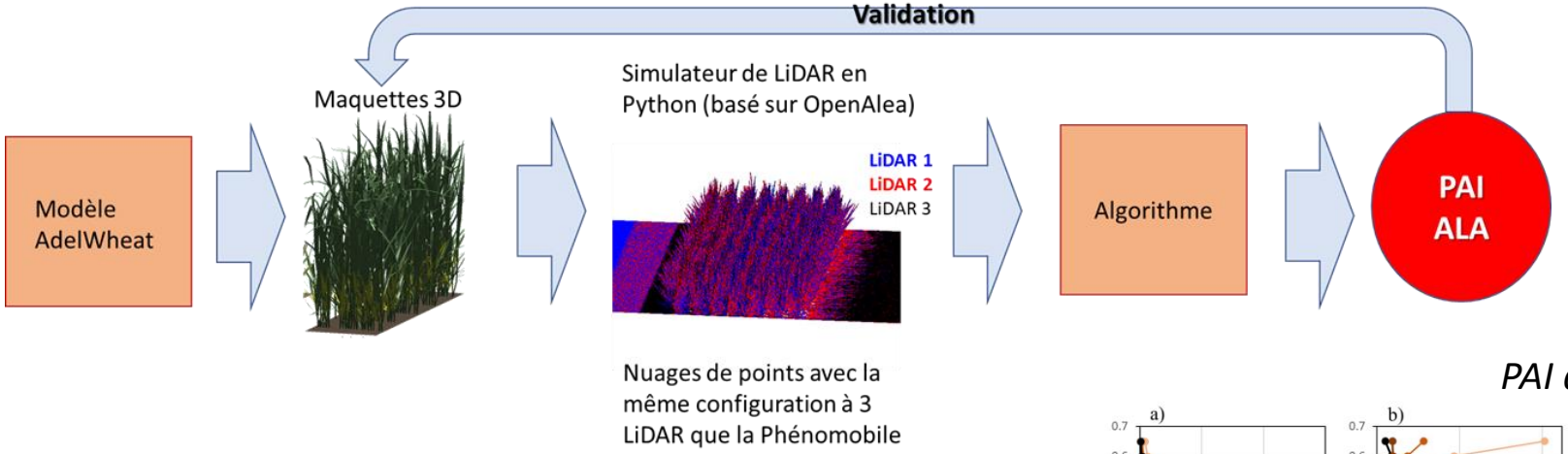

PAI and AIA at the canopy level

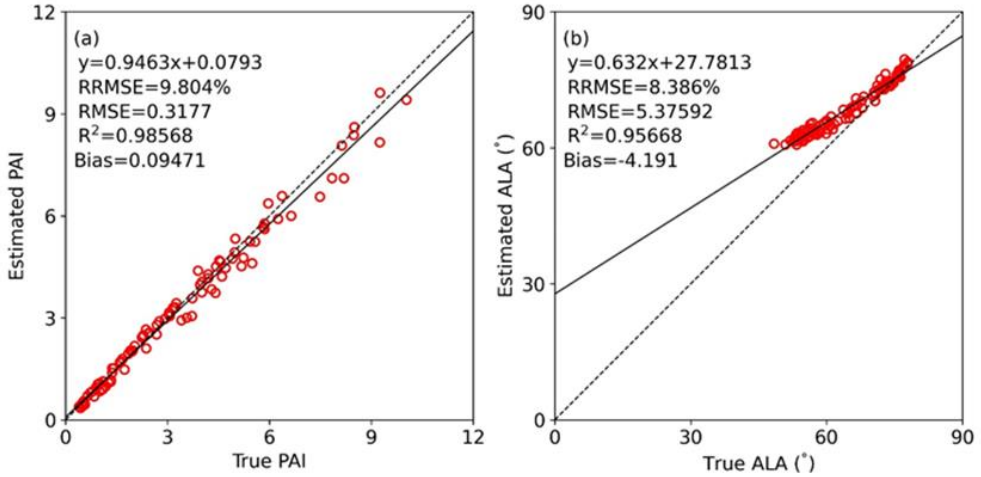

PAI and AIA at the voxel level

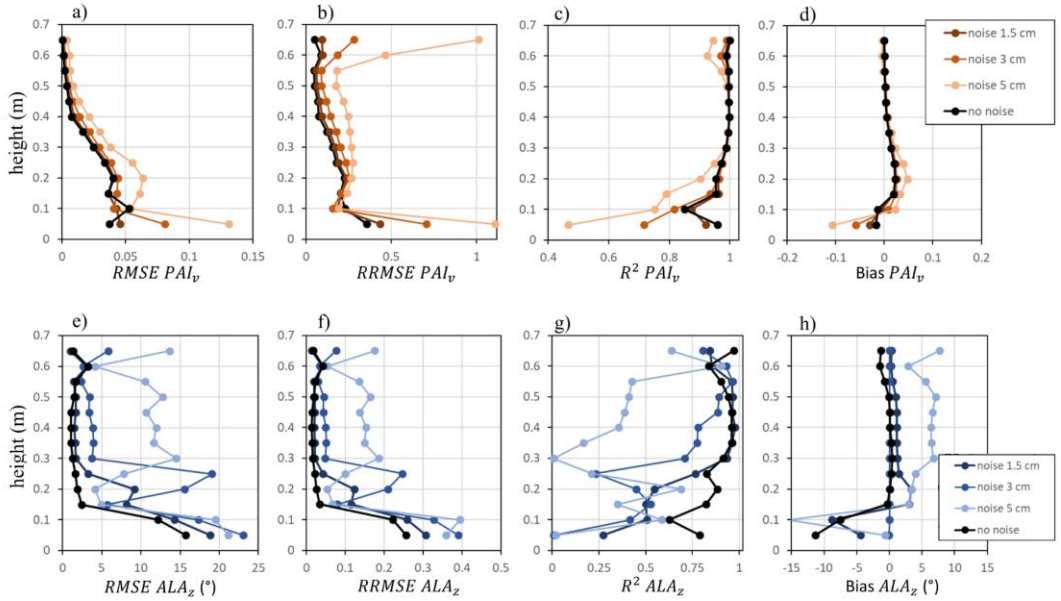

Bonus track: bias in gap fraction?

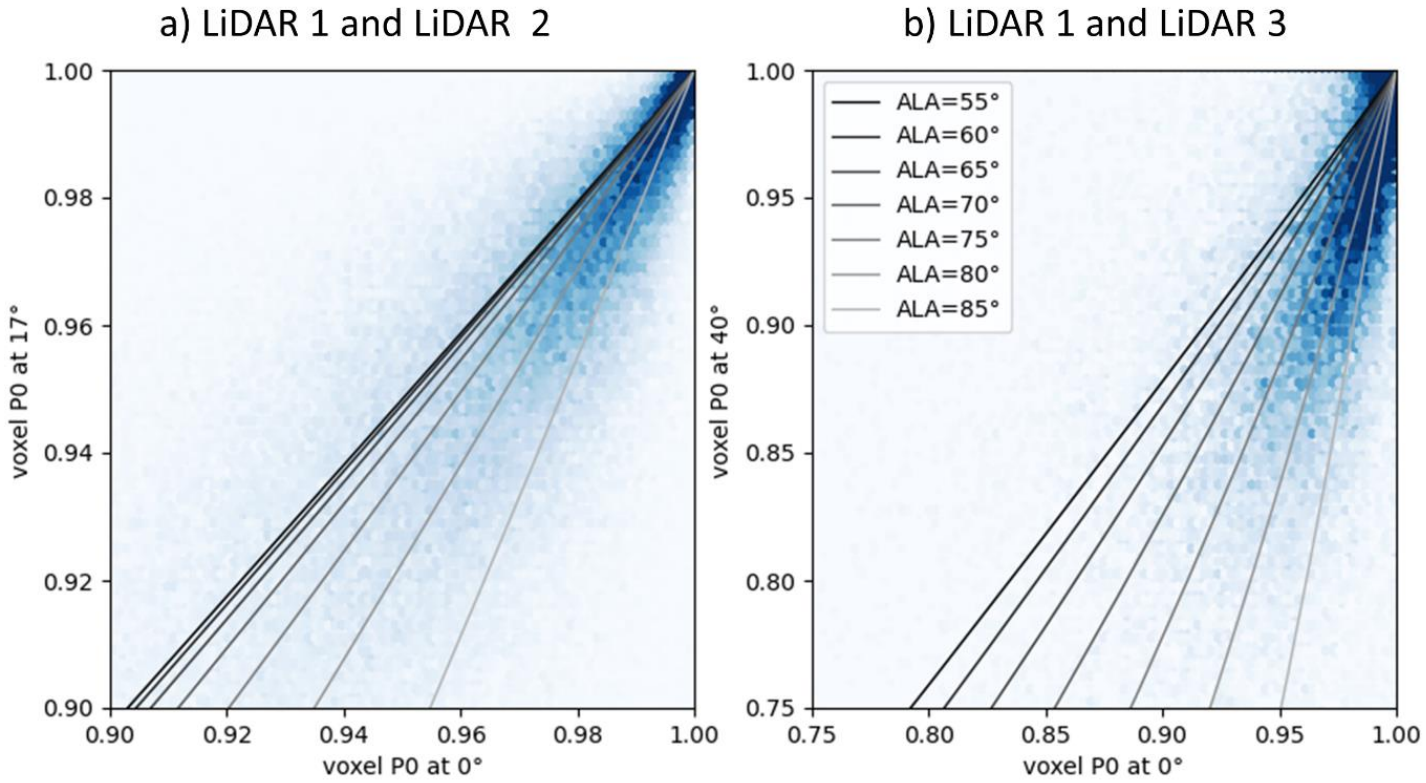

Density plots of the voxel gap fraction ($P_{0,v}$) observed simultaneously from two LiDARS at different viewing angles. The continuous lines on each graph correspond to the relationship between P_0 at the respective viewing angles predicted by Beer-Lambert law assuming different average leaf angle (AIA).